AKADÉMIAI KIADÓ

UNIVERSITY of DEBRECEN

International Review of Applied Sciences and Engineering

14 (2023) 2, 256–262

DOI:
10.1556/1848.2022.00536

ORIGINAL RESEARCH PAPER

Use of compression test to determine the Young's modulus of the titanium alloy Ti6Al4V manufactured via direct metal laser sintering

Rashwan Alkentar[1,2], Máté File[1] and Tamás Mankovits[1*]

[1] Department of Mechanical Engineering, Faculty of Engineering, University of Debrecen, Ótemető Str. 2, 4028, Debrecen, Hungary

[2] Doctoral School of Informatics, Faculty of Informatics, University of Debrecen, Kassai Str. 26, 4028, Debrecen, Hungary

Received: June 7, 2022 • Accepted: September 1, 2022
Published online: February 2, 2023

ABSTRACT

The research is dedicated to determine one of the most important mechanical properties which is the Young's modulus. Its value is crucial for clearly explaining and understanding the results of any mechanical loading experiment. Three cylindrical samples of 15 mm height and 7.5 mm diameter were designed using SpaceClaim application in the ANSYS Software and then 3D printed using Direct Metal Laser Sintering via EOS M 290 3D printer. The specimens were then tested under compression in order to determine the value of the Young's modulus for titanium alloy of grade 23 (Ti, Al, V, O, N, C, H, Fe, Y). The finite element method was executed using ANSYS mechanical to run a comparison between laboratory results with nominal results of the Young's modulus. Young's modulus value is affected by the 3D printing accuracy and quality, the material's quality as well; however, the deviation is within 10%.

KEYWORDS

3D-printing, ANSYS, Young's modulus

1. INTRODUCTION

Due to its success with the production of complicated parts, 3D printing techniques like selective laser melting (SLM) and selective laser sintering are being used with different materials and in various areas [1, 2]. In the biomedical field, 3D printing methods have the advantages in fabricating scaffolds and latticed structures with the ability to create complex shapes, geometries and porosities [3]. Bill used SLM to manufacture lattice structures used in biomedical implants in order to investigate the defects resulting from 3D printing methods in comparison to finite element analyzed models [4]. Many researches were conducted for investigating the mechanical properties of 3D printed structures.

Mazur et al. studied the compressive behavior of SLM fabricated titanium alloy structures. The research investigated various topologies sizes and geometries [5]. Direct metal laser sintering (DMLS), a 3D printing method, was used by Karolewska and Ligaj to prepare specimens of titanium alloys. The study focused on the comparison of 3D printed parts [6].

Since the Young's modulus defines the elastic behavior of the material, several attempts were reported trying to determine its value. Most of these researches investigated the Young's modulus for isotropic metallic structures because of the importance

*Corresponding author.
E-mail: tamas.mankovits@eng.unideb.hu

AKJournals

of their performance. The testing setup procedures for such a process are divided into two methods, the dynamic method like the ultrasonic measurement approach and the static method like the mechanical test (compressive, tensile) [7]. Usually, researchers used uniaxial and triaxial compression methods in order to determine the Young's modulus value [8]. The stress-strain curve does not always show a clear linear behavior with all kinds of materials, hence a single value of the Young's modulus is sometimes hard to calculate. This fact redirected the interest to the non-destructive methods which give better results regarding the elastic range [9]. K.T. Chau derived an approximate formula for calculating the Young's modulus using cylinders under compression but assuming the Poisson's ratio is already known [10].

Researchers showed that the only problem with the compression test in the modulus determination is deviated from its intrinsic value. The main reason behind this fact is the existence of friction between the upper and lower end surfaces and the loading platens [10–12]. Wei Liu suggested a correction method in his approach [13] for linear hardening materials to obtain the modulus of cylindrical specimens of aluminum using the compression test. His research showed closer values to the intrinsic modulus than the tested values. Eva Labasova, in [14], was able to determine the Young's modulus using the relative strain with predefined load conditions and universal measurement system Quantum X MX 840.

In the biomedical field, researchers focused on the modification of Young's modulus to cure stress shielding. Mitsuo proposed a study on getting the Young's modulus of titanium alloy as close to the cortical bone as possible [15]. In [16], Anders Ogaard determined the accuracy of measurements of the Young's modulus for the cancellous bone using compression testing, where the strain was measured using an extensometer attached to the compression anvils.

Pursuing reduction of the young's modulus, Yu. N. Loginov tried modifying Young's modulus value for titanium alloy Ti6Al4V used in medical implants via the finite element method analysis. Honeycomb cellular was applied as a structure for the cylindrical specimens used in the experiment. The Young's modulus was indeed reduced three times compared with the solid titanium alloy [17]. G. Rotta also studied the effect of the porous titanium alloy on its Young's modulus using the finite element method. The study showed that the pore size has a strong influence on the Young's modulus [18]. Reconstruction of the Young's modulus using the finite element method was discussed by Yanning Zhu in [19], where the approach depends on relaxing the force boundary condition requirements so that at the compression surface, only the force distribution remains. The finite element method with the help of a network of triangular elements was used to investigate the elastic properties of an isotropic composite material [20]. The finite element model updating method was discussed as a correction of the numerical model of the structure based on the measured data from the real structure [21].

In [22], Stefan derived a formula for calculating the Young's modulus using the average field approximation method in the field of composite materials. J.G. Williams [11] utilized a compression test in determining the value of Young's modulus under the assumption that radial displacement is linearly dependent on the radius of the cylindrical specimens used during the test. FE was also used to validate the results of the laboratorial tests. Jianjun proposed, in [23], the idea of determining the elastic modulus using a piezoelectric ring and electromechanical impedance. The method offered a solution for the on-site determination of mechanical properties since most of the mechanical ways required a large set of testing machines. Bucciarelli et al. [24] tried the sound waves method as a non-destructive testing way to determine the elastic modulus, where an error of 2% was achieved compared with the results of tensile-testing methods of determination. The same approach of the sound factor was used by Nunn [25].

The focus of this paper has been on the determination of the Young's modulus based on the laboratorial compression test followed by a numerical investigation using the FEM method to validate the results. The study prepares the calculation of the Young's modulus to help with an upcoming work with the same type of TI6Al4V alloy.

2. MATERIALS

Over the past few decades, titanium alloys were used in a wide range in the manufacturing of biomedical appliances. In the research, Ti6Al4V alloy of grade 23 was used in the 3D printing of the specimens. This alloy is most famous for its good biomechanical properties such as low density, high strength and high corrosion resistance that are quite necessary to enhance the osseointegration and biocompatibility in biomedical implants. The research seeks to find the exact Young's modulus for the material to generate accurate results in the laboratorial and simulative fields.

The following Table 1 shows the material's composition:

3. METHODS

3.1. CAD design and the FEM analysis

The CAD model was designed using the SpaceClaim application within the ANSYS software. The STL file was, then, exported to be processed by the 3D printing machine software. The design is a solid cylinder of height 15 mm and a diameter of 7.5 mm, as shown in Fig. 1.

The FEM analysis was applied using the mechanical application within ANSYS. The compression test was simulated in the FEM process where a force of 10 kN was

Table 1. Ti6Al4V alloy composition (based on [26])

Element	Chemical composition percentage %
Al	5.50–6.50
V	3.50–4.50
O	0.13
N	0.05
C	0.08
H	0.012
Fe	0.25
Y	0.005
Other elements each	0.1
Other element total	0.4

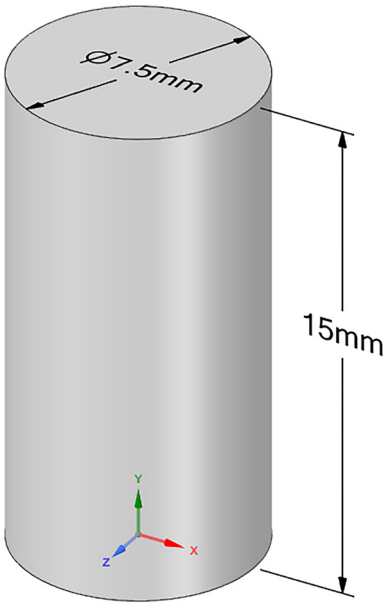

Fig. 1. The CAD design of the specimen

applied on the upper face of the cylinder. Fixed support constraint was applied on the opposite surface of the cylinder. Adaptive mesh size was chosen in order to conduct a suitable mesh for the cylinder. The following Fig. 2 shows the compression test parameters in the FEM analysis.

Depending on equation (1), the Young's modulus was calculated using stress and strain values.

$$E = \frac{\sigma}{\varepsilon} \tag{1}$$

Where E is the Young's modulus measured in MPa, σ is the stress which was calculated using the force and area of the cylinder measured in MPa, ε is the strain calculated from the change in height value.

3.2. Manufacturing

Direct metal laser sintering was used to 3D print the specimens. EOS M290 machine was used to execute the

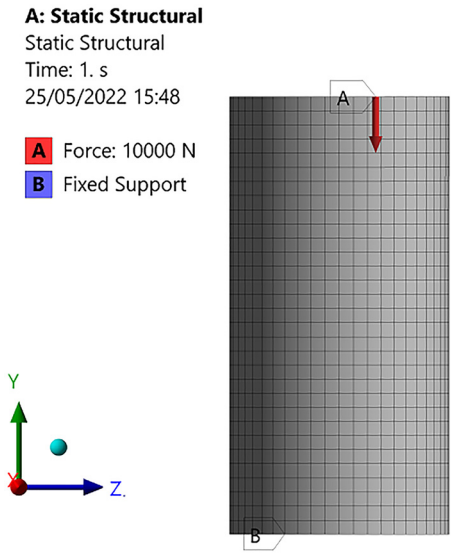

Fig. 2. The settings of the compression test simulation

manufacturing. The machine was chosen based on the characteristics that suit this type of specimen. The machine uses a laser of type Yb fiber with a 400 W power. The focus diameter is 100 µm and the scanning speed is 7 m s^{-1} [27]. EOSPRINT 2 software was used in the machine to process the CAD data. Three cylindrical samples were manufactured in total as shown in Fig. 3.

After manufacturing the samples, a digital caliper of type Mitutoyo with a precision of ±0.02 mm was used to measure the dimensions. Table 2 shows the average values of both the diameter and the height.

3.3. Compression test

The compression test was executed with INSTRON 8801 servo-hydraulic fatigue testing machine. The compression

Fig. 3. 3D-printed specimen

Table 2. Average measurements of the specimens

Specimen	Diameter [mm]	Height [mm]
1	7.458	15.22
2	7.494	14.98
3	7.486	15.09

speed was set at 1 mm min^{-1}. A video extensometer provided with a heavy-duty camera was used in order to detect the changes in displacement along the compression process. The machine is provided with the Wavematrix software as an operating system. The test was done at room temperature to avoid any confliction with the thermal expansion.

The following Fig. 4 shows one of the samples under compression. Stress-strain graphs were extracted and analyzed in order to calculate the Young's modulus of the samples.

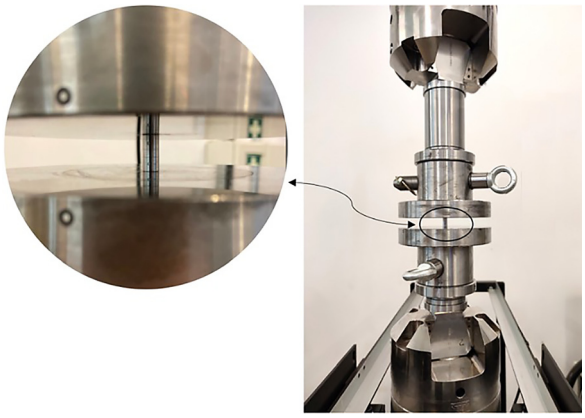

Fig. 4. Specimen under compression

4. RESULTS

4.1. Compression test

As mentioned above, the values of the strain were generated with the help of the video extensometer, which was able to record the displacement during the compression stage. Stress values were calculated based on the reaction forces values generated by the testing machine, which were applied on the cross-sectional area of the specimens.

Figure 5 shows the stress-strain results for all three specimens.

As shown in the previous figure, the Young's modulus has an average value of 106,247 MPa, which is close to the nominal value of 113,800 MPa with a deviation of 6.6%.

4.2. FEM simulation results

The calculated value of the Young's modulus taken from the laboratorial test was applied in the finite element study. The resulting deformation of the simulated compression test was recorded taking into consideration that the compression was executed in the linear range of the material only.

In order to guarantee the accuracy of the FEM solution, a deformation divergence analysis was executed on the design based on the mesh element size. Figure 6 shows how the deformation diverges with a change of less than 5%, which gives an acceptable result.

The following Fig. 7 shows the deformation distribution along the specimen. The maximum deformation shown was 0.0315 mm in response to the maximum force applied of 10 kN.

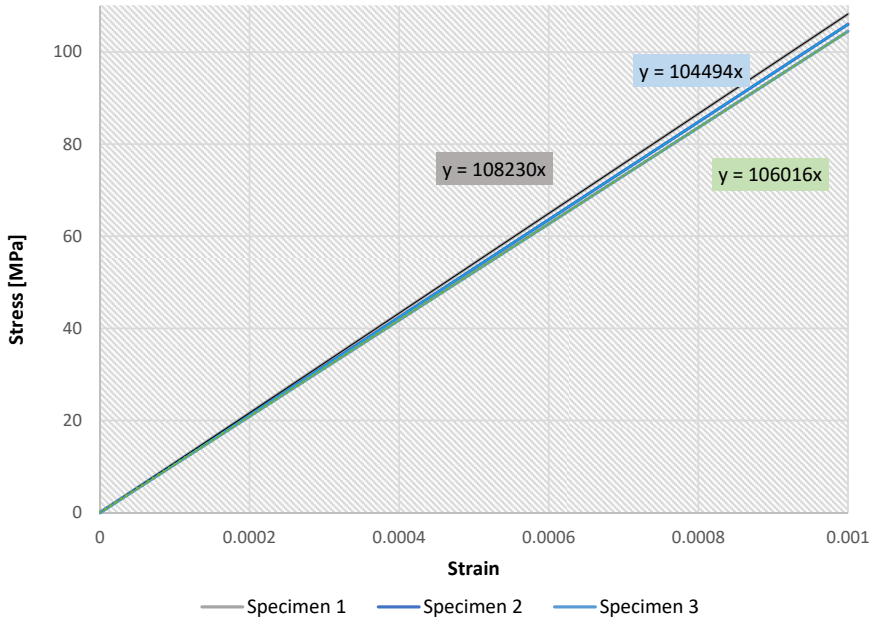

Fig. 5. Stress-strain graphs for all three specimens

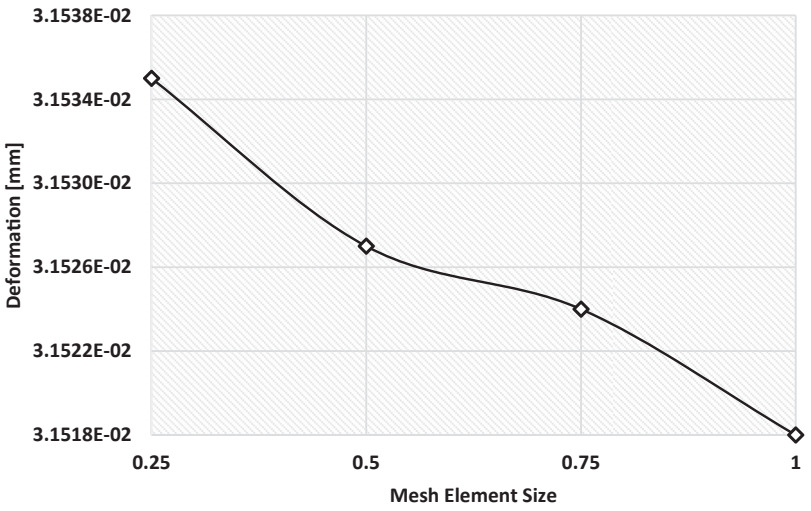

Fig. 6. Deformation divergence with mesh element size

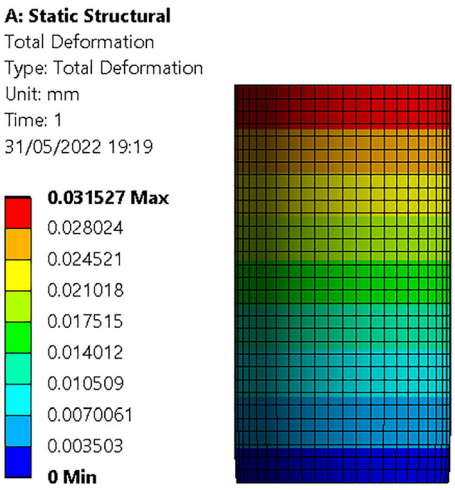

Fig. 7. Deformation within the specimen

The stress-strain graph is displayed in Fig. 8. As shown in the graph, the Young's modulus value is 108,151 MPa, which is close to the nominal known Young's modulus value of the Ti6Al4V alloy of 113,800 MPa; however, there has been a deviation of 4.9%. The average Young's modulus was shown with a value of 106,247 MPa, which represents a deviation of 1.7% from the FEM results.

5. CONCLUSIONS

Young's modulus values were investigated using a simple compression test and validated using the FEM analysis for three specimens. As seen from the results, the Young's modulus value was affected by the amount of displacement and deformation in the material. A deviation was

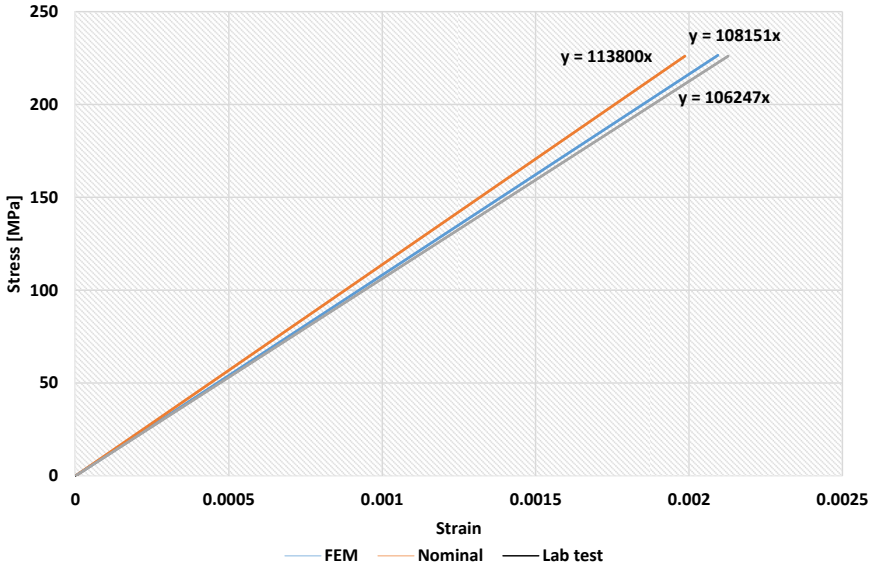

Fig. 8. Stress-strain graph

noticed from the nominal known value of the Young's modulus for the TI6Al4V alloy of grade 23 due to the following reasons:

- Printing accuracy,
- Printing quality,
- Material's quality.

Designers apply the lattice structure design on the medical implants in order to reduce the Young's modulus of the titanium alloy to a range close to that of the human bone, thus preventing the stress shielding phenomena.

Conflict of interest: The third author, Tamás Mankovits is a member of the Editorial Board of the journal. Therefore, the submission was handled by a different member of the editorial team and he did not take part in the review process in any capacity.

REFERENCES

[1] W. J. Sames, F. A. List, S. Pannala, R. R. Dehoff, and S. S. Babu, "The metallurgy and processing science of metal additive manufacturing," *Int. Mater. Rev.*, vol. 61, no. 5, pp. 315–60, Jul. 2016. https://doi.org/10.1080/09506608.2015.1116649.

[2] K. V. Wong and A. Hernandez, "A review of additive manufacturing," *ISRN Mech. Eng.*, vol. 2012, p. 208760, 2012. https://doi.org/10.5402/2012/208760.

[3] U. Jammalamadaka and K. Tappa, "Recent advances in biomaterials for 3D printing and tissue engineering," *J. Funct. Biomater.*, vol. 9, no. 1, 2018. https://doi.org/10.3390/jfb9010022.

[4] B. Lozanovski, et al., "Computational modelling of strut defects in SLM manufactured lattice structures," *Mater. Des.*, vol. 171, p. 107671, 2019. https://doi.org/10.1016/j.matdes.2019.107671.

[5] M. Mazur, M. Leary, S. Sun, M. Vcelka, D. Shidid, and M. Brandt, "Deformation and failure behaviour of Ti-6Al-4V lattice structures manufactured by selective laser melting (SLM)," *Int. J. Adv. Manuf. Technol.*, vol. 84, no. 5, pp. 1391–411, 2016. https://doi.org/10.1007/s00170-015-7655-4.

[6] K. Karolewska and B. Ligaj, "Comparison analysis of titanium alloy Ti6Al4V produced by metallurgical and 3D printing method," *AIP Conf. Proc.*, vol. 2077, no. 1, p. 20025, Feb. 2019. https://doi.org/10.1063/1.5091886.

[7] S. Suttner and M. Merklein, "A new approach for the determination of the linear elastic modulus from uniaxial tensile tests of sheet metals," *J. Mater. Process. Technol.*, vol. 241, pp. 64–72, 2017. https://doi.org/10.1016/j.jmatprotec.2016.10.024.

[8] J. Martínez-Martínez, D. Benavente, and M. A. García-del-Cura, "Comparison of the static and dynamic elastic modulus in carbonate rocks," *Bull. Eng. Geol. Environ.*, vol. 71, no. 2, pp. 263–8, 2012. https://doi.org/10.1007/s10064-011-0399-y.

[9] O. A. Quaglio, J. Margarida da Silva, E. da Cunha Rodovalho, and L. de Vilhena Costa, "Determination of Young's modulus by specific vibration of basalt and diabase," *Adv. Mater. Sci. Eng.*, vol. 2020, p. 4706384, 2020. https://doi.org/10.1155/2020/4706384.

[10] C. K. T., "Young's modulus interpreted from compression tests with end friction," *J. Eng. Mech.*, vol. 123, no. 1, pp. 1–7, Jan. 1997. https://doi.org/10.1061/(ASCE)0733-9399(1997)123:1(1).

[11] J. G. Williams and C. Gamonpilas, "Using the simple compression test to determine Young's modulus, Poisson's ratio and the Coulomb friction coefficient," *Int. J. Sol. Struct.*, vol. 45, no. 16, pp. 4448–59, 2008. https://doi.org/10.1016/j.ijsolstr.2008.03.023.

[12] R. M. Jones, "Apparent flexural modulus and strength of multi-modulus materials," *J. Compos. Mater.*, vol. 10, no. 4, pp. 342–54, Oct. 1976. https://doi.org/10.1177/002199837601000407.

[13] W. Liu, Y. Huan, J. Dong, Y. Dai, and D. Lan, "A correction method of elastic modulus in compression tests for linear hardening materials," *MRS Commun.*, vol. 5, no. 4, pp. 641–5, 2015. https://doi.org/10.1557/mrc.2015.76.

[14] E. Labašová, "Determination of modulus of elasticity and shear modulus by the measurement of relative strains," *Res. Pap. Fac. Mater. Sci. Technol. Slovak Univ. Technol.*, vol. 24, no. 39, pp. 85–92, 2017. https://doi.org/10.1515/rput-2016-0021.

[15] M. Niinomi, Y. Liu, M. Nakai, H. Liu, and H. Li, "Biomedical titanium alloys with Young's moduli close to that of cortical bone," *Regen. Biomater.*, vol. 3, no. 3, pp. 173–85, Sep. 2016. https://doi.org/10.1093/rb/rbw016.

[16] A. Odgaard and F. Linde, "The underestimation of Young's modulus in compressive testing of cancellous bone specimens," *J. Biomech.*, vol. 24, no. 8, pp. 691–8, 1991. https://doi.org/10.1016/0021-9290(91)90333-I.

[17] Y. N. Loginov, A. I. Golodnov, S. I. Stepanov, and E. Y. Kovalev, "Determining the Young's modulus of a cellular titanium implant by FEM simulation," *AIP Conf. Proc.*, vol. 1915, no. 1, p. 30010, Dec. 2017. https://doi.org/10.1063/1.5017330.

[18] G. Rotta, T. Seramak, and K. Zasińska, "Estimation of Young's modulus of the porous titanium alloy with the use of fem package," *Adv. Mater. Sci.*, vol. 15, no. 4, pp. 29–37, 2015. https://doi.org/10.1515/adms-2015-0020.

[19] Y. Zhu, T. J. Hall, and J. Jiang, "A finite-element approach for Young's modulus reconstruction," *IEEE Trans. Med. Imaging*, vol. 22, no. 7, pp. 890–901, 2003. https://doi.org/10.1109/TMI.2003.815065.

[20] B. O. Jaensson and B. O. Sundström, "Determination of Young's modulus and Poisson's ratio for WC-Co alloys by the finite element method," *Mater. Sci. Eng.*, vol. 9, pp. 217–22, 1972. https://doi.org/10.1016/0025-5416(72)90036-5.

[21] F. Adel, S. Shokrollahi, and E. Beygi, "Determination of Young's modulus by finite element model updating TT - تعیین مدول یانگ با روش به-روزرسانی مدل المان محدود," *mdrsjrns*, vol. 19, no. 8, pp. 1837–44, Aug. 2019, [Online]. Available: http://mme.modares.ac.ir/article-15-20783-en.html.

[22] Š. Barta, "Effective Young's modulus and Poisson's ratio for the particulate composite," *J. Appl. Phys.*, vol. 75, no. 7, pp. 3258–63, Apr. 1994. https://doi.org/10.1063/1.356132.

[23] J. Wang, W. Li, C. Lan, and P. Wei, "Effective determination of Young's modulus and Poisson's ratio of metal using piezoelectric ring and electromechanical impedance technique: a proof-of-concept study," *Sensors Actuators A. Phys.*, vol. 319, p. 112561, 2021. https://doi.org/10.1016/j.sna.2021.112561.

[24] F. Bucciarelli, G. P. Malfense Fierro, M. Zarrelli, and M. Meo, "A non-destructive method for evaluation of the out of plane

elastic modulus of porous and composite materials," *Appl. Compos. Mater.*, vol. 26, no. 3, pp. 871–96, 2019. https://doi.org/10.1007/s10443-018-9754-5.

[25] J. Nunn, "Measuring Young's modulus the easy way, and tracing the effects of measurement uncertainties," *Phys. Educ.*, vol. 50, no. 5, pp. 538–47, 2015. https://doi.org/10.1088/0031-9120/50/5/538.

[26] U.S Titanium industry, "Titanium alloys - Ti6Al4V Grade 5," 2002. https://www.azom.com/article.aspx?ArticleID=1547. Accessed: Jun. 25, 2022.

[27] EOS.info, "Technical data EOS M 290," 2022. https://www.eos.info/en/additive-manufacturing/3d-printing-metal/eos-metal-systems/eos-m-290. Accessed: Jun. 25, 2022.